DELPHI Collaboration DELPHI 2001-024 CONF 465
7 March, 2001

Measurement of the W-pair Production Cross-section and W Branching Ratios at $\sqrt{s} = 205$ and 207 GeV

Preliminary results for the 2001 Moriond Conference

DELPHI Collaboration

P.Buschmann[1], M.Calvi[2], R.Chierici[3], G.Gomez-Ceballos[4], D. Jeans[5], F.Matorras[4], U.Mueller[1], M.Paganoni[2], C.Parkes [6], P.Renton[5], J.Timmermans[7] A.Tonazzo[2], H.Wahlen[1], G.Wilkinson[5]

Abstract

The cross-section for the process $e^+e^- \to W^+W^-$ was measured with the data sample collected by DELPHI at centre-of-mass energies up to 209 GeV and corresponding to a total integrated luminosity of about 209 pb^{-1}. Dividing the data into two centre-of-mass energy ranges, the following results were obtained:

$$\begin{aligned} \sigma_{WW}(205 \text{ GeV}) &= 17.44 \pm 0.60 \text{ (stat)} \pm 0.22 \text{ (syst) pb} \\ \sigma_{WW}(207 \text{ GeV}) &= 16.50 \pm 0.43 \text{ (stat)} \pm 0.21 \text{ (syst) pb} \end{aligned}$$

The branching ratios of the W decay were also measured.

[1]Fachbereich Physik, University of Wuppertal, Postfach 100 127, D-42097 Wuppertal, Germany
[2]Dipartimento di Fisica, Università di Milano Bicocca, p.za della Scienza 3, I-20126 Milan, Italy
[3]CERN, CH-1211 Geneva 23, Switzerland
[4]Instituto de Fisica de Cantabria (CSIC-UC), Avda. los Castros s/n, ES-39006 Santander, Spain
[5]Department of Physics, University of Oxford, Keble Road, Oxford OX1 3RH, UK
[6]Department of Physics, University of Liverpool, P.O. Box 147, Liverpool L69 3BX, UK
[7]NIKHEF, Postbus 41882, NL-1009 DB Amsterdam, The Netherlands

1 Introduction

In this note we present preliminary results on the cross-section for the doubly resonant production of W bosons measured with the data sample collected in 2000 by DELPHI.

LEP delivered data at energies up to 209 GeV. The data are divided into two centre-of-mass energy ranges, above and below 205.5 GeV, referred to as 205 GeV and 207 GeV in the following. The luminosity-weighted centre-of-mass energies and the amount of data collected at each energy are reported in table 1. The sum of the luminosities corresponds to about 209 pb^{-1}; its systematic error is estimated to be $\pm 0.6\%$, dominated by the experimental uncertainty of the Bhabha measurements of $\pm 0.5\%$. The luminosities used for different selections correspond to those data for which all elements of the detectors essential to the specific analysis were fully functional.

$\mathcal{L}$-weighted $\sqrt{s}$ (GeV)	Hadronic $\mathcal{L}$ (pb^{-1})	Leptonic $\mathcal{L}$ (pb^{-1})
204.9	73.42	66.30
206.7 TPC OK	85.54	80.63
206.7 TPC-S6 off	49.50	49.09

Table 1: Energies and luminosities in 2000.

One of the TPC sectors (S6) was not operational during the last period of the high energy data taking. These data were analysed separately and then combined with the results from the previous period. The performance of the analyses were found to be compatible within statistical errors. Additional systematics effects were estimated by comparing the data collected at the Z peak during the period with the TPC-S6 off with simulation samples produced with the same detector conditions. Both hadronic and leptonic Z decays were used. The impact on the WW cross-section analysis was conservatively evaluated as an uncertainty on the selection efficiency of 0.5% in the fully hadronic channel and of 1% in the other channels, which was added to the systematic error.

The criteria for the selection of WW events generally follow those used for the cross-section measurements at lower energies [1]. Event selections are briefly reviewed in section 2. In section 3 the total cross-section and the branching fractions of the W boson are presented.

The cross-sections determined in this analysis correspond to W pair production through the three doubly resonant tree-level diagrams ("CC03 diagrams" [2]) involving s-channel γ and Z exchange and t-channel ν exchange. Depending on the decay mode of each W, fully hadronic, mixed hadronic-leptonic ("semileptonic") or fully leptonic final states are obtained. The Standard Model branching fractions are 45.6%, 43.9% and 10.5%, respectively. The EXCALIBUR [3] four-fermion generator interfaced with the full DELPHI simulation program DELSIM [4, 5] was used to produce signal Montecarlo events. The selection efficiencies were defined with respect to the CC03 diagrams only by reweighting the events to the CC03 contribution according to the ratio of the squared matrix elements computed with these diagrams only and with the full set of diagrams.

2 Event selection and cross-sections

2.1 Fully hadronic final state

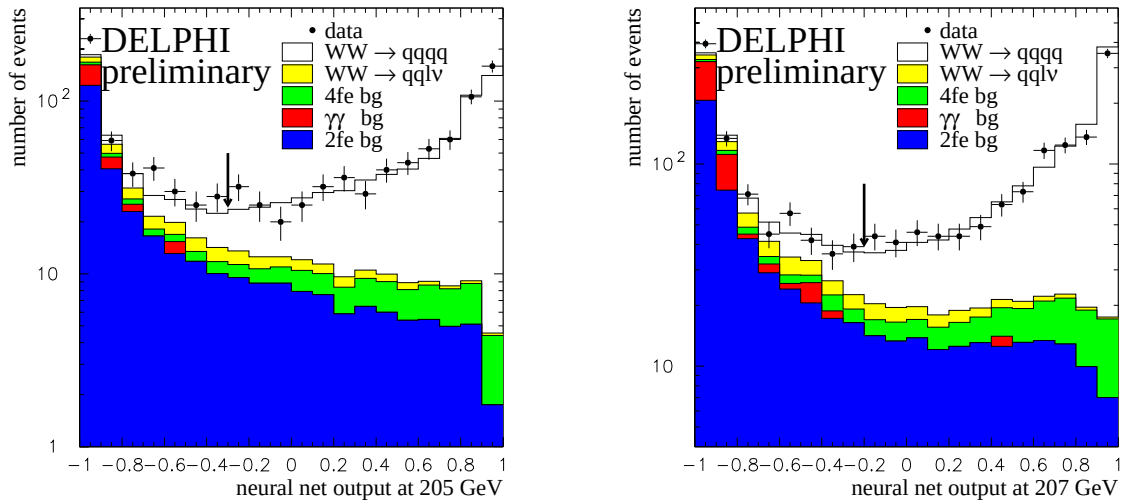

Figure 1: Distribution of the Neural Net output variable for 4-jet events at the centre-of-mass energy of 205 GeV (left) and 207 GeV (right). The points show the data and the histograms are the predicted distributions for signal and background. The arrows indicate the cut value applied for the selection of events.

A feed forward neural network was used to separate $W^+W^- \to q\overline{q}q\overline{q}$ events from 2-fermion (mainly $Z^0/\gamma \to q\overline{q}$) and 4-fermion background (mainly ZZ). The network is based on the JETNET package [6] and uses the back-propagation algorithm. The input variables were observables related to the effective centre-of-mass energy $\sqrt{s'}$ [7], to the four-jet topology, to the event shape, and the probability from a constrained fit imposing the W mass; a detailed list is given in [8], where the network architecture is also described.

After loose preselection cuts ($\sqrt{s'} > 140$ GeV, 4 or more jets clustering with DURHAM [9] and $y_{min} = 0.0015$, jet multiplicity ≥ 3) the training of the feed forward net was performed with 2500 events from signal (EXCALIBUR MC) and as many Z^0/γ events (PYTHIA [10] MC). The network output was then calculated for independent samples of simulated events and for the real data. Figure 1 shows the output distribution of the neural network for data and MC.

Events were selected by applying a cut on the NN output parameter, chosen by optimising the product of efficiency and purity of the selection at each energy. The overall selection efficiency at 205 GeV was $(85.5 \pm 0.8)\%$. The cross-section for the expected total background, including semileptonic WW decays, was estimated to be (1.77 ± 0.10) pb. For both periods of the high centre-of-mass energy the selection efficiency and the backgrounds were found to be consistent with the ones at 205 GeV.

The total number of events selected in each data sample is reported in table 2.

The cross-section for fully hadronic events was obtained from a binned maximum likelihood fit to the distribution of the NN output variable, taking into account the partial efficiency and the expected background in each bin. The results for

	efficiencies for selected channels			
channel	$jjjj$	$jje\nu$	$jj\mu\nu$	$jj\tau\nu$
$q\bar{q}q\bar{q}$	0.855	$< 10^{-4}$	$< 10^{-4}$	0.005
$q\bar{q}e\nu$	0.017	0.701	0.002	0.074
$q\bar{q}\mu\nu$	0.008	0.003	0.852	0.030
$q\bar{q}\tau\nu$	0.050	0.022	0.021	0.587
background (pb)	1.57	0.208	0.047	0.491
$\sqrt{s}$ (GeV)	Selected events			
205	661	142	143	129
207	1134	222	274	301

Table 2: Data for the cross-section measurement of the hadronic and semileptonic final states. The efficiency matrix and the background are the ones at 205 GeV. The backgrounds include two-fermion and non CC03 four-fermion contributions. The upper limits on the efficiencies close to zero are at 95% C.L.

$\sigma_{WW}^{qqqq} = \sigma_{WW}^{tot} \times$ BR $(WW \to q\bar{q}q\bar{q})$, where BR$(WW \to q\bar{q}q\bar{q})$ is the probability for the WW pair to give a purely hadronic final state, are reported in table 3. The systematic errors include contributions from efficiency and background determination and from luminosity measurement; in addition, uncertainties due to fragmentation modelling were accounted for by assuming a 5% error on the QCD background, as in [8].

$\sqrt{s}$ (GeV)	$\sigma_{WW}^{qqqq} = \sigma_{WW}^{tot} \times \mathrm{BR}(WW \to q\bar{q}q\bar{q})$ (pb)
205	8.48 ± 0.40 (stat) ± 0.09 (cor.syst) ± 0.05 (unc.syst)
207	7.70 ± 0.29 (stat) ± 0.09 (cor.syst) ± 0.04 (unc.syst)

Table 3: Measured hadronic cross-sections. The first error is statistical, the second is the part of the systematic uncertainty correlated between the measurements at the two centre-of-mass energies, the last is the uncorrelated part of the systematic error.

2.2 Semileptonic final state

Events in which one of the W bosons decays into $l\nu$ and the other one into quarks are characterised by two hadronic jets, one isolated lepton (coming either directly from the W decay or from the cascade decay $W \to \tau\nu \to e\nu\nu\nu$ or $\mu\nu\nu\nu$) or a low multiplicity jet due to a τ decay, and missing momentum resulting from the neutrino(s). The major background comes from $q\bar{q}(\gamma)$ production and from four-fermion final states containing two quarks and two leptons of the same flavour.

Four channels were considered: $q\bar{q}\mu\nu$, $q\bar{q}e\nu$, 'hadronic' $q\bar{q}\tau\nu$, and 'single prong' $q\bar{q}\tau\nu$. The structure of each selection was similar: after a loose preselection, an Iterative Dis-

criminant Analysis (IDA) [11] was used to make the final selection. The IDA was trained on Montecarlo samples generated at a centre-of-mass energy of 206 GeV: 60k signal events, 46k $q\bar{q}(\gamma)$ events, and smaller samples (of 15k events) of $q\bar{q}ll$ ($l = e, \mu, \tau$) final states produced with EXCALIBUR. It was then tested on independent simulation samples. Two examples of the IDA output distribution are shown in figure 2. Events were selected with a cut on the output of the IDA, chosen to optimise the product of efficiency and purity for each channel.

2.2.1 $q\bar{q}\mu\nu$ selection

The event was required to have at least one particle identified as a muon. In the case of more than one tagged μ, the one with the largest value of $p \cdot \theta_{iso}$, where p is the momentum and θ_{iso} the isolation angle with respect to the closest charged track above 1 GeV/c, was considered to be the μ candidate. All other particles in the event were forced into two jets using the DURHAM algorithm.

The momentum of the candidate muon was required to be greater than 17 GeV/c, and a cut was made on the quality of the two forced jets: each should contain at least 4 particles, at least one of them charged. In order to reduce background from two photon processes, the transverse energy of the event (defined as $\sum_{tracks} |p_T|$) was required to exceed 40 GeV, and the visible energy to exceed 60 GeV. Events which failed a 2C kinematic fit were rejected.

An IDA selection with 2 degrees and 2 steps was then applied, using the following 9 variables:
- μ momentum p_μ;
- μ isolation angle;
- magnitude of the missing momentum p_{miss};
- polar angle of p_{miss};
- angle between p_μ and p_{miss};
- smaller of the two μ – forced jet angles;
- mass from a 2C fit;
- transverse energy of event;
- ratio of the reconstructed effective centre-of-mass energy and the true centre-of-mass energy $\sqrt{s'}/\sqrt{s}$.

2.2.2 $q\bar{q}e\nu$ selection

The event was required to have at least one particle identified as an electron and not to have been selected as $q\bar{q}\mu\nu$. In the case of more than one tagged e, the candidate was selected with the same criteria used for the $q\bar{q}\mu\nu$ channel. All other particles in the event were forced into two jets with the DURHAM algorithm.

The energy of the candidate electron was required to be greater than 20 GeV/c, and its polar angle between 23° and 157°. The same cut on the quality of the forced jets made in the $q\bar{q}\mu\nu$ selection was applied, and the transverse energy of the event was required to exceed 50 GeV. The event was rejected if it failed a 2C kinematic fit.

An IDA selection with 2 degrees and 3 steps was then applied, using 10 variables:
- electron energy;

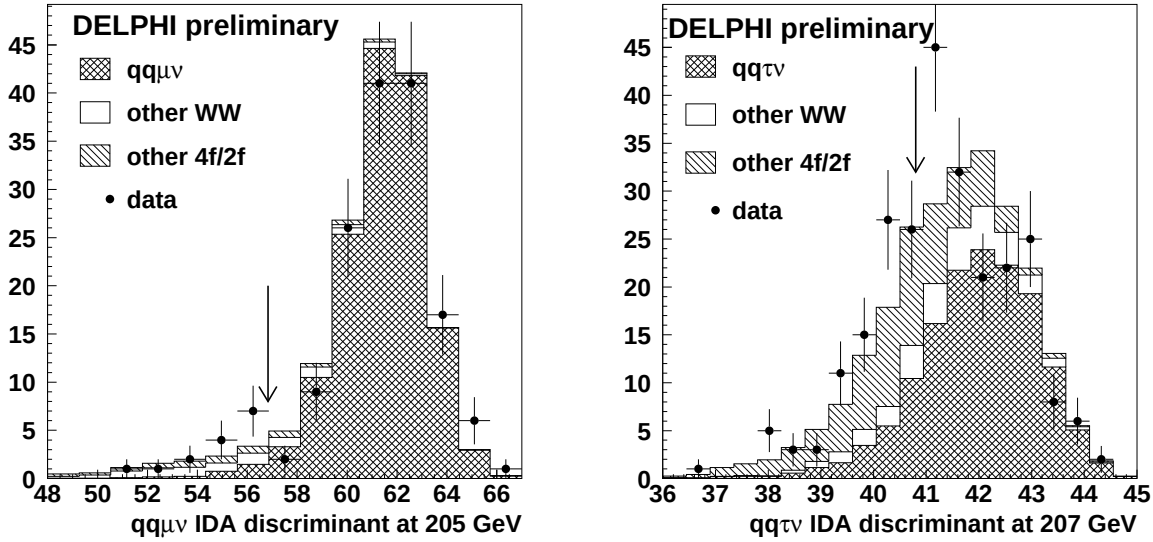

Figure 2: Distributions of the IDA discriminants in the $q\bar{q}\mu\nu$ channel at a centre-of-mass energy of 205 GeV (left) and in the 'hadronic' $q\bar{q}\tau\nu$ channel at 207 GeV (right). The arrows show where the cuts were made.

- electron isolation angle;
- magnitude of the missing momentum p_{miss};
- polar angle of p_{miss};
- angle between electron momentum and p_{miss};
- smaller of the two electron – forced jet angles;
- angle between the two forced jets;
- mass from a 2C fit;
- visible energy of event;
- $\sqrt{s'}/\sqrt{s}$.

2.2.3 'Hadronic' $q\bar{q}\tau\nu$ selection

The event was required not to be selected as $q\bar{q}e\nu$ or $q\bar{q}\mu\nu$. All the particles in the event were clustered into jets using the LUCLUS [12] algorithm with a value of d_{join} of 6.5 GeV/c. Jets with a momentum of at least 5 GeV/c, containing no more than ten particles and between one and five charged particles were considered to be τ candidates. In the case of several candidates, the one with smallest momentum weighted spread, defined as $\sum_i(\theta_i \cdot |p_i|)/\sum_i |p_i|$, where θ_i is the angle made by the momentum p_i of the i^{th} particle in the jet with the total jet momentum, was chosen.

All other particles were forced into two jets with the DURHAM algorithm. The two forced jets were required to satisfy the same conditions as in the electron and muon channels. The transverse energy was required to be above 40 GeV. Events which failed a 1C kinematic fit were rejected.

An IDA selection with 2 degrees and 3 steps was then applied, using 12 variables:
- magnitude of τ momentum p_τ;
- multiplicity of τ jet;

- hadronic energy of τ jet;
- electromagnetic energy of τ jet;
- magnitude of p_{miss};
- polar angle of p_{miss};
- smaller of the two τ – forced jet angles;
- angle between two forced jets;
- mass from 1C fit;
- visible energy of event;
- multiplicity of event;
- $\sqrt{s'}/\sqrt{s}$.

2.2.4 'Single prong' $q\bar{q}\tau\nu$ selection

The event was required not to be accepted in any of the previous semileptonic selections. The total number of particles in the event was required to be less than 50. Events with a visible energy greater than 175 GeV were rejected, as were those with a transverse energy smaller than 40 GeV.

The charged track with the highest value of $p \cdot \theta_{iso}$ was chosen as the lepton candidate. All other particles were forced into two jets. The chosen track was required to have a momentum between 5 and 45 GeV/c, and the quality of the two forced jets was assessed in the same way as in the other semileptonic selections.

An IDA selection with 2 degrees and 3 steps was then applied using 11 variables:
- polar angle of prong;
- isolation angle of prong;
- magnitude of p_{miss};
- polar angle of p_{miss};
- angle between the two forced jets;
- event thrust;
- event sphericity;
- event multiplicity;
- visible energy;
- transverse energy;
- $\sqrt{s'}/\sqrt{s}$.

Events were considered as $q\bar{q}\tau\nu$ candidates if they passed the .OR. of the 'Hadronic' and the 'Single prong' selections.

2.2.5 Results on semileptonic events

The efficiency matrix and background contamination for the semileptonic event selection were evaluated independently at the different centre-of-mass energies and found to differ by at most 2%. The values at 205 GeV are reported in table 2. The total efficiency on semileptonic WW events was $(76.4 \pm 1.3)\%$ (77.7% for e, 88.5% for μ and 63.0% for τ events), and the total expected background was (0.75 ± 0.05) pb. The errors include all the systematic uncertainties, assumed to be equal to the ones at 189 GeV [8], except for the ones described in the Introduction and in section 3. Table 2 also shows the number of selected events at each energy.

$\sqrt{s}$ (GeV)	$\sigma_{WW}^{qql\nu} = \sigma_{WW}^{tot} \times \mathrm{BR}(WW \to q\bar{q}l\nu)$ (pb)
205	7.10 ± 0.41 (stat) ± 0.13 (cor.syst) ± 0.03 (unc.syst)
207	7.08 ± 0.29 (stat) ± 0.12 (cor.syst) ± 0.03 (unc.syst)

Table 4: Measured semileptonic cross-sections. The first error is statistical, the second is the part of the systematic uncertainty correlated between the measurements at the two centre-of-mass energies, the last is the uncorrelated part of the systematic error.

A total of 1211 events were selected as semileptonic W decays; the number of events observed in the different lepton channels was found to be consistent with lepton universality. With the values given in table 2 and assuming lepton universality, a likelihood fit yields the cross sections $\sigma_{WW}^{qql\nu} = \sigma_{WW}^{tot} \times \mathrm{BR}(WW \to q\bar{q}l\nu)$ reported in table 4. The systematic errors include contributions from efficiency, background determination and luminosity measurement.

2.3 Fully leptonic final state

Events in which both W bosons decay into $l\nu$ are characterised by low multiplicity, by a clean two-jet topology with two energetic, acollinear and acoplanar leptons of opposite charge and by large missing momentum and energy.

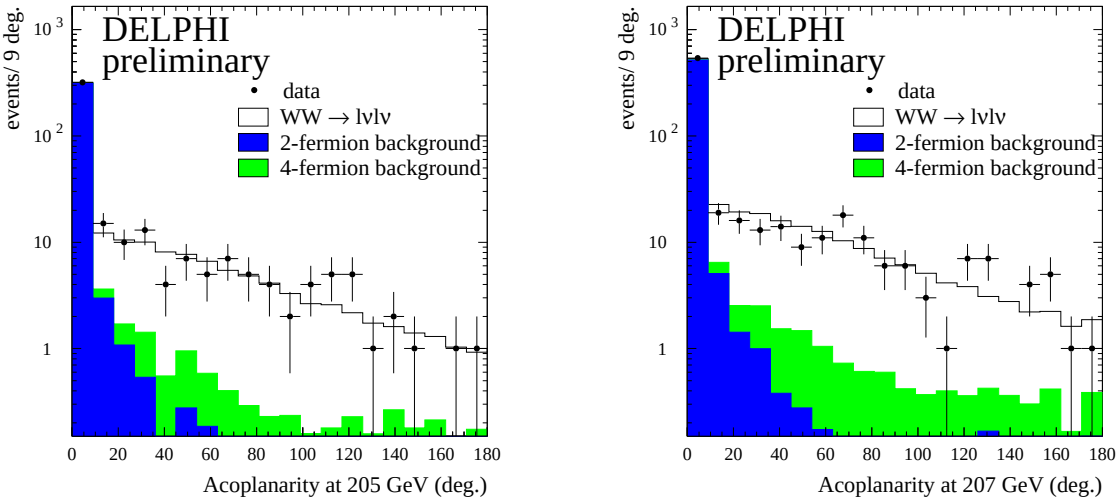

Figure 3: Distribution of the acoplanarity angle for fully-leptonic events at the 2000 centre-of-mass energies. The points show the data and the histograms are the predicted distributions for signal and background.

The selection was performed in three steps. First a leptonic event preselection was applied, described in detail in [8]. After the preselection, each jet was identified as either a μ, e or hadron (the latter therefore considered as a τ). Different cuts involving the transverse momentum in the event, its acoplanarity and acollinearity were then applied, being tighter for those sub-channels, like $e\nu e\nu$, $e\nu\tau\nu$ and $\tau\nu\tau\nu$, where more background is expected.

The distribution of the acoplanarity angle, after having applied all cuts except the one on the acoplanarity, is shown in Figure 3.

The efficiencies and backgrounds for the selection at 205 GeV are reported in table 5, together with the number of observed events in the data sets at the different energies. The overall efficiency for a flavour-blind selection was $(60.0 \pm 1.5)\%$. The residual background from non-WW events is (0.134 ± 0.032) pb.

	efficiencies for selected channels					
channel	$\tau\nu\tau\nu$	$e\nu\tau\nu$	$\mu\nu\tau\nu$	$e\nu e\nu$	$e\nu\mu\nu$	$\mu\nu\mu\nu$
$\tau\nu\tau\nu$	0.254	0.067	0.073	0.005	0.008	0.005
$e\nu\tau\nu$	0.070	0.388	0.008	0.041	0.040	$< 2 \cdot 10^{-3}$
$\mu\nu\tau\nu$	0.040	0.004	0.476	$< 2 \cdot 10^{-3}$	0.056	0.037
$e\nu e\nu$	0.022	0.138	$< 10^{-3}$	0.402	$< 10^{-3}$	$< 2 \cdot 10^{-3}$
$e\nu\mu\nu$	0.011	0.044	0.087	$< 2 \cdot 10^{-3}$	0.560	$< 10^{-3}$
$\mu\nu\mu\nu$	0.004	$< 10^{-3}$	0.088	$< 2 \cdot 10^{-3}$	0.003	0.609
background (pb)	0.027	0.027	0.017	0.028	0.015	0.020
$\sqrt{s}$ (GeV)	Selected events					
205	11	17	15	8	23	6
207	8	26	41	14	43	13

Table 5: Data for the cross-section measurement of the fully leptonic final state. The efficiency matrix and the background are the ones at 205 GeV. The upper limits on the efficiencies close to zero are at 95% C.L.

With the values of selected events, efficiencies and backgrounds at the different centre-of-mass energies, and assuming lepton universality, a likelihood fit yields the cross-sections reported in table 6. The systematic error has contributions from the efficiency and background determination and from the measurement of the luminosity.

$\sqrt{s}$ (GeV)	$\sigma_{WW}^{\ell\nu\ell\nu} = \sigma_{WW}^{tot} \times \mathrm{BR}(WW \to \ell\nu\ell\nu)$ (pb)
205	1.71 ± 0.22 (stat) ± 0.05 (cor.syst) ± 0.05 (unc.syst)
207	1.69 ± 0.16 (stat) ± 0.04 (cor.syst) ± 0.04 (unc.syst)

Table 6: Measured fully-leptonic cross-sections. The first error is statistical, the second is the part of the systematic uncertainty correlated between the measurements at the two centre-of-mass energies, the last is the uncorrelated part of the systematic error.

3 Determination of total cross-section and branching fractions

The total cross-section for WW production and the W leptonic branching fractions were obtained from a likelihood fit based on the probabilities of finding the observed number of events in each final state. The input numbers in the form given in tables 2 and 5 were used, except for the fully hadronic final state, where the binned distribution of the neural network output was used.

From all the final states combined, the branching fractions shown in table 8 were obtained. The correlation matrix is reported as well. The results are consistent with lepton universality. The fit was repeated, assuming lepton universality; the result for the hadronic branching fraction is also given in table 8, and is in agreement with the Standard Model prediction of 0.675.

The measurement of the branching fractions obtained combining the present data with the one at lower centre-of-mass energies [1, 8, 13, 14, 15] are summarised in table 9.

Assuming the other parameters of the Standard Model, i.e. $|V_{ud}|$, $|V_{us}|$, $|V_{ub}|$, $|V_{cd}|$, $|V_{cb}|$ of the CKM matrix, lepton couplings to W bosons, and the strong coupling constant α_s, to be fixed to the values given in [16], the measured hadronic branching fraction can be converted into

$$|V_{cs}| = 1.003 \pm 0.019 \text{ (stat)} \pm 0.016 \text{ (syst)},$$

where the uncertainties on the Standard Model parameters are included in the systematic error.

The total cross-sections for WW production, with the assumption of Standard Model values for the branching fractions, are reported in table 7.

$\sqrt{s}$ (GeV)	σ^{tot}_{WW} (pb)
205	17.44 ± 0.60 (stat) ± 0.21 (cor.syst) ± 0.07 (unc.syst)
207	16.50 ± 0.43 (stat) ± 0.20 (cor.syst) ± 0.06 (unc.syst)

Table 7: Measured total WW cross-sections. The first error is statistical, the second is the part of the systematic uncertainty correlated between the measurements at the two centre-of-mass energies, the last is the uncorrelated part of the systematic error.

For completeness, the measurements of the total cross-section obtained from the two periods of the high-energy data taking with the TPC-S6 on and off were:

$$\sigma^{tot}_{WW} = 16.73 \pm 0.54 \text{ (stat)} \pm 0.20 \text{ (corr.syst)} \pm 0.07 \text{ (unc.syst) pb} \quad \text{TPC OK}$$
$$\sigma^{tot}_{WW} = 16.10 \pm 0.70 \text{ (stat)} \pm 0.20 \text{ (corr.syst)} \pm 0.11 \text{ (unc.syst) pb} \quad \text{TPC-S6 off}$$

where the first error is statistical, the second is the part of the systematic uncertainty correlated between the two periods, and the third is the uncorrelated part. The contribution to the systematics due to TPC-S6 amounts to 0.092 pb.

The preliminary results on 2000 data and the previous DELPHI cross-section measurements at the lower energies [1, 8, 13, 14, 15] are shown in figure 4. They are compared with the most recent calculations in double pole approximation (DPA) from RacoonWW [17]

and YFSWW [18]. As DPA computations are not reliable close to the WW threshold, the predictions below 168 GeV were obtained by replacing DPA with a calculation in improved Born approximation, which only accounts for initial state radiation and Coulomb corrections. The shaded region represents the theoretical uncertainty of the calculations and is obtained by an analytic parametrisation of the relative uncertainty given in [19]. This leads to an accuracy on the theoretical curves of about 0.7% at 168 GeV and of 0.4% at 200 GeV. The uncertainty from RacoonWW and from YFSWW have been then merged into a single error band.

To account for systematic effects, not yet investigated in detail, due to the more precise computation of the radiative corrections in DPA, a further conservative systematic error was added to the measurements. This corresponds to a relative variation of the selection efficiency of 0.5% [20]. The published and preliminary DELPHI measurements are in very good agreement with the Standard Model expectations.

Acknowledgements

We are greatly indebted to our technical collaborators, to the members of the CERN-SL Division for the excellent performance of the LEP collider, and to the funding agencies for their support in building and operating the DELPHI detector.

channel	branching fraction	stat. error	syst. error	syst. from QCD bkg
$W \to e\nu$	0.1039	0.0054	0.0017	0.0004
$W \to \mu\nu$	0.1046	0.0046	0.0010	0.0004
$W \to \tau\nu$	0.1041	0.0066	0.0026	0.0003

Correlations	$W \to e\nu$	$W \to \mu\nu$	$W \to \tau\nu$
$W \to e\nu$	1.00	-0.06	-0.32
$W \to \mu\nu$	-0.06	1.00	-0.23
$W \to \tau\nu$	-0.32	-0.23	1.00

	assuming lepton universality			
channel	branching fraction	stat. error	syst. error	syst. from QCD bkg
$W \to$ hadrons	0.6873	0.0072	0.0033	0.0010

Table 8: W branching fractions from 2000 data and correlation matrix for the leptonic branching fractions. The uncertainty from the QCD background (column 5) is included in the systematic error (column 4).

channel	branching fraction	stat. error	syst. error	syst. from QCD bkg
$W \to e\nu$	0.1036	0.0030	0.0016	0.0005
$W \to \mu\nu$	0.1062	0.0026	0.0010	0.0005
$W \to \tau\nu$	0.1099	0.0039	0.0026	0.0003

Correlations	$W \to e\nu$	$W \to \mu\nu$	$W \to \tau\nu$
$W \to e\nu$	1.00	-0.05	-0.33
$W \to \mu\nu$	-0.05	1.00	-0.25
$W \to \tau\nu$	-0.33	-0.25	1.00

	assuming lepton universality			
channel	branching fraction	stat. error	syst. error	syst. from QCD bkg
$W \to$ hadrons	0.6810	0.0041	0.0032	0.0012

Table 9: W branching fractions from the DELPHI data above the WW production threshold and correlation matrix for the leptonic branching fractions. The uncertainty from the QCD background (column 5) is included in the systematic error (column 4).

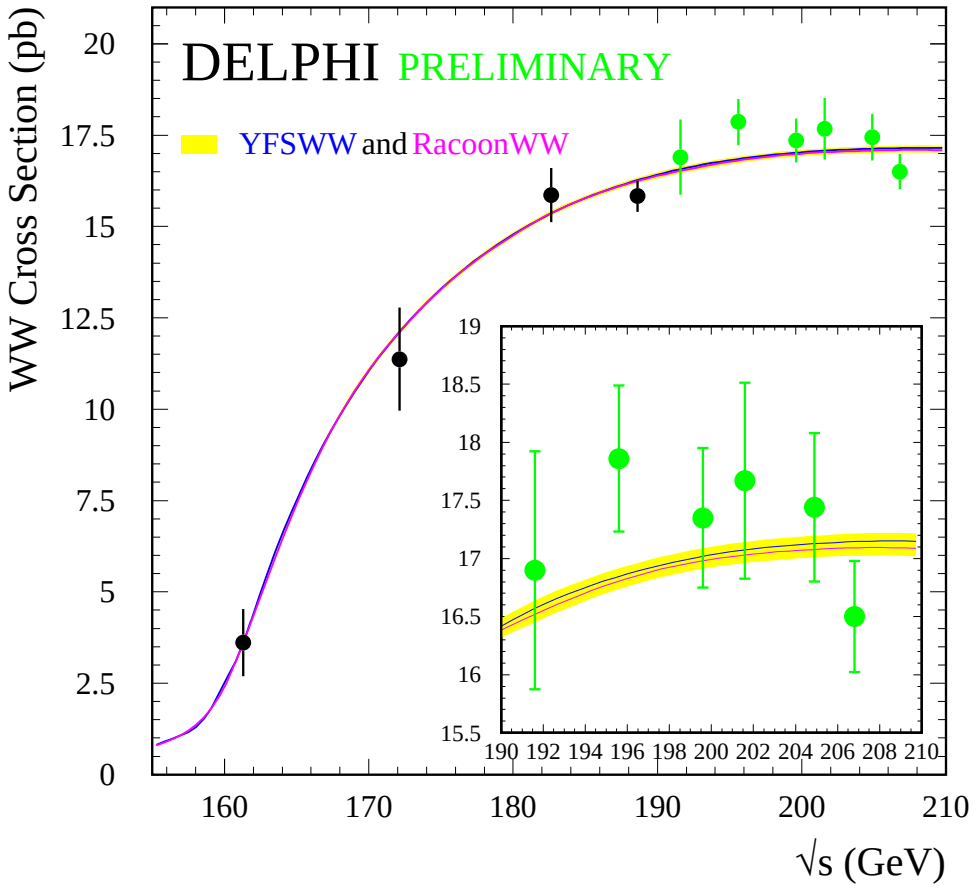

Figure 4: Measurements of the W^+W^- cross-section compared with the Standard Model prediction given by the YFSWW [18] and RacoonWW [17] programs. The shaded band represents the uncertainty on the theoretical calculations.

References

[1] DELPHI Collaboration, *Measurement of the W-pair production cross-section and W branding ratios at* $\sqrt{(s)} = 192-202$ *GeV*, DELPHI Note 2000-140 CONF 439 (2000), contributed paper to ICHEP2000, Osaka.

[2] W. Beenakker, F. A. Berends et al., *WW Cross-Section and Distributions*, Physics at LEP2, eds. G. Altarelli, T. Sjöstrand and F. Zwirner, CERN 96-01 (1996) Vol 1, 79.

[3] F. A. Berends, R. Kleiss, R. Pittau, *EXCALIBUR*, Physics at LEP2, eds. G. Altarelli, T. Sjöstrand and F. Zwirner, CERN 96-01 (1996) Vol 2, 23.

[4] DELPHI Collaboration: P. Abreu et al., Nucl. Instr. and Meth. **A378** (1996) 57.

[5] DELPHI Collaboration, *DELPHI event generation and detector simulation - User Guide*, DELPHI Note 89-67 (1989), unpublished.

[6] L.Lønnblad, C.Peterson, H.Pi, T.Røgnvaldsson
JETNET *3.1 - A Neural Network program for jet discrimination and other High Energy Physics triggering situations*
Department of Theoretical Physics, University of Lund, Sweden (1994).

[7] P. Abreu et al, Nucl. Instr. and Meth. **A427** (1999) 487.

[8] DELPHI Collaboration, P.Abreu et al., Phys. Lett. **B479** (2000) 89.

[9] S. Catani et al., Phys. Lett. **B269** (1991) 432.

[10] T. Sjöstrand, *PYTHIA 5.719 / JETSET 7.4*, Physics at LEP2, eds. G. Altarelli, T. Sjöstrand and F. Zwirner, CERN 96-01 (1996) Vol 2, 41.

[11] T.G.M. Malmgren, Comp. Phys. Comm. **106** (1997) 230.

[12] T. Sjöstrand, *PYTHIA 5.7 / JETSET 7.4*, CERN-TH.7112/93 (1993).

[13] DELPHI Collaboration, P.Abreu et al., Phys. Lett. **B456** (1999) 310.

[14] DELPHI Collaboration, P.Abreu et al., E. Phys. J. **C2** (1998) 581.

[15] DELPHI Collaboration, P.Abreu et al., Phys. Lett. **B397** (1997) 158.

[16] Particle Data Group, E. Phys. J. **C15** (2000) 1.

[17] A. Denner et al., Phys. Lett. **B475** (2000) 127.

[18] S. Jadach et al., **hep-ph/0007012**.

[19] Four-Fermion Working Group Report: *Four-Fermion Production in Electron-Positron Collisions*, **hep-ph/0005309**.

[20] Results presented at the *"WWMM workshop"* in Sesimbra, Portugal, 1-4 November 2000.